



HAL
open science

Insulin aggregation starts at dynamic triple interfaces, originating from solution agitation

Karim Chouchane, Thibaut Frachon, Laurent Marichal, Laurent Nault,
Charlotte Vendrely, Antoine Maze, Franz Bruckert, Marianne Weidenhaupt

► **To cite this version:**

Karim Chouchane, Thibaut Frachon, Laurent Marichal, Laurent Nault, Charlotte Vendrely, et al..
Insulin aggregation starts at dynamic triple interfaces, originating from solution agitation. *Colloids
and Surfaces B: Biointerfaces*, 2022, 10.1016/j.colsurfb.2022.112451 . hal-03663284

HAL Id: hal-03663284

<https://hal.science/hal-03663284>

Submitted on 10 May 2022

HAL is a multi-disciplinary open access archive for the deposit and dissemination of scientific research documents, whether they are published or not. The documents may come from teaching and research institutions in France or abroad, or from public or private research centers.

L'archive ouverte pluridisciplinaire **HAL**, est destinée au dépôt et à la diffusion de documents scientifiques de niveau recherche, publiés ou non, émanant des établissements d'enseignement et de recherche français ou étrangers, des laboratoires publics ou privés.

Insulin aggregation starts at dynamic triple interfaces, originating from solution agitation

Karim Chouchane^{a,1}, Thibaut Frachon^{a,1}, Laurent Marichal^a, Laurent Nault^a, Charlotte Vendrely^{a,b}, Antoine Maze^a, Franz Bruckert^a, Marianne Weidenhaupt^{a*}

¹ common first authors

* corresponding author

^a Université Grenoble Alpes, CNRS, Grenoble-INP*, LMGP, F-38000 Grenoble, France

^b CY Cergy Paris University, ERRMECe, I-MAT (FD4122), F-95000 Neuville sur Oise, France

* Institute of Engineering Univ. Grenoble Alpes

Emails:

KC: dr.karim.chouchane@gmail.com

TF: thibaut.frachon@free.fr

LM: laurent.marichal@grenoble-inp.fr

LN: laurent.nault@orange.fr

CV: charlotte.vendrely@grenoble-inp.fr

AM: antoine.maze@grenoble-inp.fr

FB: franz.bruckert@grenoble-inp.fr

MW: marianne.weidenhaupt@grenoble-inp.fr

Corresponding author: Marianne Weidenhaupt

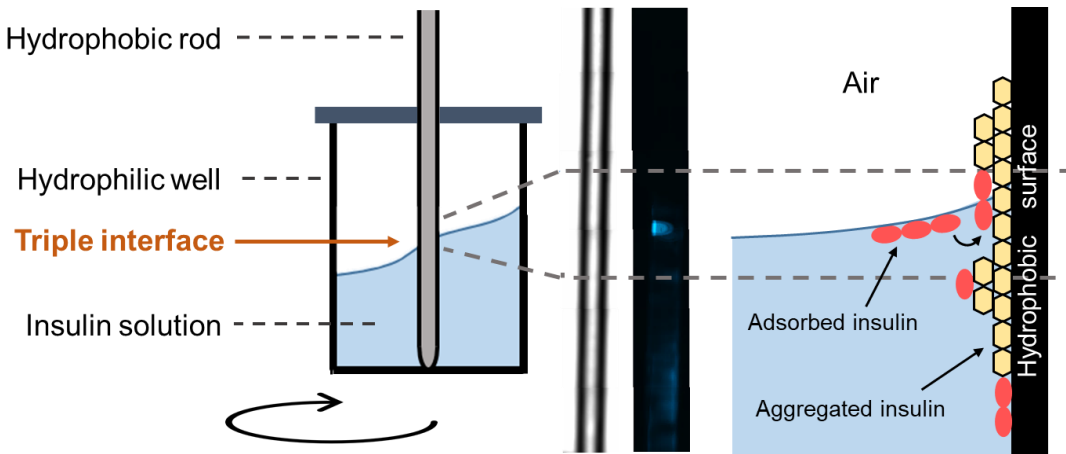
Tel: +33 4 56 52 93 35

Postal address: Grenoble INP - Minatec

3 parvis Louis Néel - CS 50257

38016 Grenoble cedex 1, France

Graphical abstract



Abstract

The consequences of agitation on protein stability are particularly relevant to therapeutic proteins. However, the precise contribution of the different effects induced by agitation in pathways leading to protein denaturation and aggregation at interfaces is not entirely understood. In particular, the contribution of a moving triple line, induced by the sweeping of a solution meniscus on a container wall upon agitation, has only been rarely assessed.

In this article, we therefore designed experimental setups to analyze how mixing, shear stress, and dynamic triple interfaces influence insulin aggregation in physiological conditions. This has been achieved by controlling agitation speed, shear stress, and the extension of triple interfaces in order to shed light on the contribution of different agitation-induced effects on insulin aggregation in physiological conditions.

We demonstrate that strong agitation is necessary for the onset of insulin aggregation, while the growth of the aggregates is sustained even under weak agitation. Kinetic insulin aggregation studies in conditions of intermittent wetting show that the aggregation rate correlates with the amount of dynamic triple interfaces that the proteins are exposed to. Finally, we demonstrate that the triple line, where the protein solution, the air, and a hydrophobic surface meet constitutes a preferential early aggregation site.

Keywords: protein stability, interfacial adsorption, protein aggregation, agitation, triple interface, protein dehydration, insulin

Introduction

Advances in biotechnology have enabled engineering and large scale production of proteins, leading to a rapid development of protein-based therapeutics in recent years [1–3]. However, proteins are inherently unstable and numerous physicochemical parameters can affect their conformation and ultimately their bioactivity [4]. Among these, protein adsorption at interfaces and their concomitant aggregation has been identified as a major challenge facing the pharmaceutical industry [5–7]. Indeed, proteins are constantly exposed to solid material, air, and liquid interfaces during their production, storage, and delivery. Moreover, the growing automation of production, purification, and administration protocols has increased the impact of interfaces combined with mechanical stresses on the stability of therapeutic proteins (i.e. the tendency for a protein to maintain its native structure). For example, during automated purification protocols, a protein solution is pumped through chromatography columns and filter membranes, exposing the proteins in flow conditions to column, filter materials, and air [8].

Material surfaces, especially hydrophobic ones, are well known to induce protein adsorption, conformational changes, and aggregation [9–13]. The air-solution interface also presents hydrophobic properties, promoting protein adsorption and aggregation [14–16]. By contrast with an air-solution interface, within which adsorbed proteins can move to a certain extent, proteins are fixed when adsorbed on a solid hydrophobic material. Therefore, mechanical stresses, induced by liquid flow over a surface or by stirring, can affect surface-adsorbed proteins in several ways. When submitted to a hydrodynamic flow, surface-adsorbed proteins and especially high molecular weight aggregates can get fragmented and detach from the surface [17]. This not only leads to protein aggregates in solution but can also sustain the formation of surface-induced aggregation by re-exposing formerly covered surface to the solution or by creating secondary aggregation nucleation sites [18–20]. Agitation of a protein solution in a container in the presence of air creates a dynamic triple line, where the air-liquid interface meets the solid surface. Indeed, upon shaking or stirring, the solution meniscus moves up and down the container wall, thus creating a triple interface zone that is transiently wet and dry. Surface-adsorbed proteins in this zone are therefore exposed to partial dehydration which can induce their aggregation [21].

Insulin is a small globular protein used for the treatment of diabetes mellitus. Its stability has been extensively studied in various conditions (low pH and high temperature [22], physiological conditions [23]). It has also been known for a long time for its aggregation into amyloid fibrils

[24] and its instability in medical devices [25,26]. At physiological pH and temperature, it has been shown by Sluzky and colleagues [23] and then by Ballet and coworkers [27] that a solution of human insulin can aggregate in the presence of a hydrophobic surface only when the solution is agitated. In this case, insulin surface-adsorption and the subsequent formation of aggregation nuclei on the hydrophobic surface are responsible for a fast protein aggregation. Without agitation or in the absence of a hydrophobic surface, insulin is stable for days [27].

Agitation induces mixing, hydrodynamic shear stress, and the creation of a dynamic triple line where surface-adsorbed proteins can be exposed to air. Each of these agitation-induced effects contributes to the kinetics of insulin aggregation at hydrophobic surfaces, but their individual importance might differ at various time points during aggregation. We have therefore designed several experimental setups containing hydrophobic surfaces and air, to shed light on agitation-induced molecular mechanisms and their impact on insulin aggregation. We show that a critical level of agitation is necessary for the **onset** of hydrophobic surface-induced insulin aggregation in physiological conditions and that aggregate growth is sustained, even at low levels of agitation. We also demonstrate, using intermittent wetting on beads, that insulin aggregation is enhanced by the creation of dynamic triple interfaces. Finally, we report that early insulin aggregates form preferentially at the dynamic triple line.

Materials and methods

Chemicals

Recombinant human insulin produced in yeast, dichlorodimethylsilane, and Thioflavin T (ThT) were purchased from Sigma-Aldrich (ref: I2643, 440272, and T3516, respectively). Poly(L-Lysine) (20 kDa) grafted with Polyethylene Glycol (5 kDa) (PLL-PEG) was purchased from SuSoS (ref: PLL(20)-g[3.5]-PEG(5)). Insulin stock solutions were prepared at a concentration of around 1 mg/mL (172 μ M) in TN buffer (Tris-HCl 25 mM, NaCl 125 mM, pH 7.4). 1M HCl was added to completely dissolve insulin in the buffer at pH 3.2, then 1M NaOH was added to adjust the final pH back to 7.4. The concentration was adjusted by UV absorbance at 280 nm using an extinction coefficient of 5.53 $\text{mM}^{-1} \text{cm}^{-1}$. ThT stock solutions were prepared in TN buffer at a concentration of 1 mM, adjusted by absorbance measurement (1% ThT in ethanol, $\epsilon_{416\text{nm}}(\text{ThT}) = 26.6 \text{mM}^{-1} \text{cm}^{-1}$). All solutions were stored at 4°C, conserved less than two weeks and filtered through a 0.22 μm Millex-GV filter unit from Merck Millipore (ref: SLGV033SS) before use.

Kinetic analyses

In this manuscript the term “aggregate” is used for insulin oligomers/assemblies that can be measured by positive ThT-fluorescence or solution turbidity (optical density at 600 nm). Such aggregates can be found in solution and also adsorbed on interfaces. The insulin aggregation kinetics proceeded in three phases: a lag phase, where the signal was not statistically different from the baseline (mean \pm standard deviation), a linear growth phase and a plateau phase. Experimentally, the lag time was defined as the first point where the signal exceeds the mean + 3 times the standard deviation of the baseline ($OD_{600} > 0.045$). Growth slopes were calculated on three consecutive OD_{600} data points and the maximum growth slope was calculated during the kinetics. The plateau was defined as the maximum OD_{600} attained. The maximum growth slope was normalized to the plateau value to define the growth rate $k(\omega)$, expressed in $\% \cdot h^{-1}$. These parameters were calculated on individual kinetics corresponding to different samples, and the given statistics represent the average and the standard deviation for each parameter. The number of independent experiments and of samples in each experiment, as well as the analysis of the data is indicated in Supplementary Materials.

Transparent polystyrene microplates (diameter = 6.6 mm) (Greiner Bio One flat bottom ref: 655101) and black polystyrene microplates (Nunc F96 MicroWell polystyrene nontreated flat-bottom, Thermo Fisher Scientific (ref: 237105)) were used for optical density and ThT fluorescence measurements, respectively. Insulin was used at 86 μ M with 20 μ M ThT. The plates were covered by plastic sheets, incubated at 37°C and shaken at different rotation speeds ω (Heidolph Titramax, 1.5 mm vibration orbit). Turbidity (OD at 600 nm) or bound ThT fluorescence ($\lambda_{ex} = 450$ nm; $\lambda_{em} = 482$ nm) were measured at the indicated time with a Tecan M1000[®] spectrophotometer.

Surface functionalization

Two types of functionalized surfaces were used: PEGylated (hydrophilic, uncharged), and silanized (hydrophobic) surfaces. Glass beads (diameter: 1 mm \pm 10 %, Sigma-Aldrich ref: Z273619) and glass rods (diameter: 1 mm \pm 10 %, GoodFellow ref: SI817910) were first washed and etched with 14.5 M NaOH solution for 5 min under agitation, then thoroughly rinsed with deionized water. After this treatment the surfaces became negatively charged.

Some glass rods were functionalized with PLL-PEG (PLL(20)-g[3.5]- PEG(5), SuSoS). The protocol given by the supplier was adapted as follow: after NaOH etching, the rods received an oxygen-plasma treatment (2 min), then were placed in non-binding tubes, and incubated in a PLL-PEG solution (0.2 g.L^{-1}) dispersed in HEPES buffer (10 mM, NaCl 150 mM, pH 7.4) for 30 minutes. Samples were then cleaned with pure water, dried, and stored in an argon-filled tube. In order to assess the level of hydrophobicity, some glass coverslips underwent the same treatment and their water contact angle was measured at $35.6^\circ \pm 6.9^\circ$, in agreement with similar PEG functionalizations [28].

Silanization of glass beads and rods was performed after NaOH etching and oxygen-plasma treatment by immersing in dichlorodimethylsilane 5% (v/v) in toluene solution for 2 hours. Finally, after cleaning with ethanol and water, curing was done by placing the beads and rods at 120°C for 2h. Water contact angle measured on glass coverslips that underwent the same treatment was $116.1^\circ \pm 11.0^\circ$, indicating a significant hydrophobicity [29].

Insulin aggregation at triple interfaces on beads

In order to create dynamic triple solid-liquid-air interfaces, an insulin solution is repeatedly moved up and down a layer of hydrophobic beads inside a column. When the liquid is withdrawn, triple interfaces are created between the bead surfaces and the meniscus of the solution. A scheme of the setup is presented in **Figure 1**. A 1 mL solution of $86 \mu\text{M}$ insulin and $20 \mu\text{M}$ ThT was degassed during 10 minutes using a Laboport vacuum pump (KNF Neuberger). A chromatography column (empty Micro Bio-Spin column, BioRad ref: 732-6204) was filled with 300 mg of previously functionalized hydrophobic glass beads (about 150 beads). Then, a 5 mL syringe was filled with 1 mL of the degassed solution and connected to the chromatography column with tubing (Masterflex ref: Tygon Lab E-3603 L/S 14). The volume inside the column, when the syringe piston is pushed at its limit, is 0.5 mL. The syringe was placed on a syringe pump, which was programmed to repeatedly withdraw (pulling the piston back) the protein solution from the column and then immerse (pushing the piston forward) the beads with the solution. The flow rate was set to 4 mL.min^{-1} and the displaced volume was 0.5 mL. The column was closed with a cap pierced with two needles to avoid overpressure and evaporation. The whole system is put in an incubator at 37°C alongside with a beaker full of water to saturate the atmosphere with water vapor.

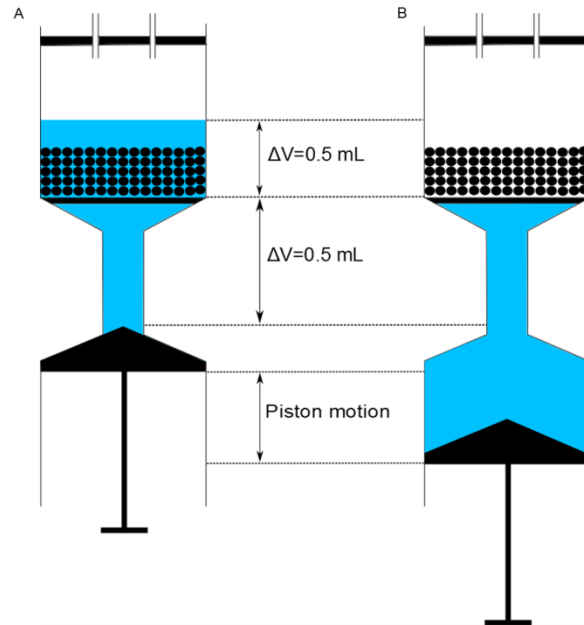


Figure 1: Scheme of the experimental setup creating triple interfaces on beads. A syringe (bottom) fills a column (top), which contains 300 mg of hydrophobic glass beads, with an insulin solution. The solution is represented in blue, the piston and the column bed support (beneath the beads) in black, and the beads by black disks. The syringe is fixed on a syringe pump (not shown). The displaced volume is $\Delta V = 0.5 \text{ mL}$ and the flow rate is $4 \text{ mL}\cdot\text{min}^{-1}$.

A, beads are immersed in the insulin solution.

B, the insulin solution is withdrawn from the column so that the air-liquid interface moves through the bead layer, thus creating triple interfaces at the bead surfaces.

Two experiments with different conditions were conducted in parallel for a direct comparison of the aggregation kinetics. After 4 hours of incubation, 200 μL of solution was taken from the columns at every hour, put in a 96 microwell plate and ThT fluorescence was measured on a Tecan infinite M1000 spectrophotometer ($\lambda_{\text{ex}} = 450 \text{ nm}$; $\lambda_{\text{em}} = 482 \text{ nm}$). After the fluorescence measurement, the solution was put back into the column. The measurement error was determined by calculating the maximal standard deviation of ThT values, measured at the same experimental time points, in five independent experiments with identical conditions. The ThT fluorescence background signal ($10.4 \pm 1.8 \text{ A.U.}$), measured for a fresh and filtered 86 μM insulin solution containing 20 μM ThT, was subtracted. Therefore, the indicated fluorescence values can be attributed to the presence of ThT-positive aggregates.

Insulin aggregation on a hydrophobic glass rod

In order to visualize early onsets of aggregation, a setup of rods plunged into an insulin solution was developed. Hydrophilic multiwell plates were used (PEGylated surface, ref: Corning 3651).

A silicon-sealed plate cover with holes where rods can be fitted at the center of each well, was designed. To prevent evaporation, the holes not in use were sealed by a plate film. Each well contained 250 μL of insulin (86 μM) and ThT (20 μM) solution in TN buffer. Rods (either PEGylated or silanized) were plunged in each well, then the covered plate was agitated at 1200 rpm (Heidolph Titramax, 1.5 mm vibration orbit) at 37°C for various durations. After incubation, total ThT fluorescence was measured in each well and the glass rods were placed on a sample-holder, precisely fixing their position for comparison purpose. Rods were imaged in air on a Zeiss Axio-Observer 7 inverted microscope through a 4x magnification objective both under bright field and by episcopic illumination at the ThT excitation wavelength. The microscope was fitted with a Colibri 7 solid-stat light source and a BP 390/40_{ex}, BP 450/40_{em} filter cube. Images were recorded using an 8-bit Zeiss Axiocam 506 mono camera. Fluorescence profiles along the rod axis were analyzed using the “Plot Profile” function of the ImageJ software [30]. Normalization of the fluorescence profiles was performed for each rod by subtracting the mean fluorescence intensity of the area of the rod that is never immersed.

Results

Effect of agitation speed on insulin aggregation kinetics in multiwell plates

Agitation is an important parameter that controls the kinetics of insulin aggregate formation. Here, we varied the agitation speed of a hydrophobic multiwell plate containing insulin solutions on an orbital shaker in order to analyze its effect on insulin aggregation. Optical density (OD₆₀₀) was used to monitor the aggregation kinetics.

Due to the inertia of the liquid, there is a threshold rotation speed, below which the liquid does not move independently from the well it is contained in [31]. In such conditions no vortex is formed and agitation-induced mixing does not occur. We determined that the threshold rotation speed for 200 μL of solution in a 96-well plate on our orbital shaker is 600 rpm (details in Materials and Methods). Below this speed, the mixing is not effective and molecules move mainly by diffusion. Above 600 rpm, the mixing frequency is sufficient to reach an efficient mixing [31,32]. In terms of insulin aggregation this translates into the impossibility to measure lag times below 600 rpm (**Figure 2A**) meaning that no aggregation onset occurred during the duration of the experiment. It should be noted that in the absence of agitation, insulin solutions

remain stable for weeks, even in the presence of hydrophobic surfaces [23]. Between 600 and 700 rpm, the insulin aggregation lag time decreases sharply and, above 700 rpm, the lag time reaches a minimum at around 2h. This indicates that the aggregation speed is maximized at this mixing speed and stronger agitation does not make it faster. Agitation causes two phenomena: (1) mixing, that increases the surface adsorption rate of insulin molecules by ensuring a constant concentration of insulin near the material surface, and (2) hydrodynamic shear stress, that may increase desorption of insulin from surfaces as well as fragmentation of aggregates [20]. In the absence of agitation, insulin molecules move mainly by diffusion which is insufficient to allow an efficient build-up of insulin nuclei on the material surface (**Figure 2**, grey zones). Therefore, mixing is likely to be the driving force during the nucleation phase (lag phase) while shear stress does not seem to influence early steps of insulin aggregate formation.

In contrast, the agitation speed increases the aggregation growth rate (Figure 2B). This figure combines two sets of data, obtained in different ways. At rotation speeds higher than 600 rpm, the insulin solution was continuously agitated at the indicated speed (Figure 2B, black squares). Interestingly, once aggregation has started, the agitation speed can be reduced down to 100 rpm, because the fluid mechanical properties have changed (the inertia is now able to overcome the surface tension). To study the aggregation growth rate in the range 0-600 rpm, hydrophobic multiwell plates were filled with insulin solutions and agitated at 1200 rpm during the lag time, then they were further agitated at different indicated rotation speeds, and the aggregation kinetics was recorded using OD_{600} (Figure 2B, white squares). Put together, these data show that there is a continuous increase of the growth rate with the rotation speed (Figure 2B). Fitting the experimental data $k(\omega)$ with a power law (Figure 2B, solid line) shows that the growth rate increases as the $3/2$ power of the rotation speed ω (equation 1 $k_{th}(\omega) = A \omega^{3/2}$, see Supplementary Materials). Since under laminar flow conditions, the average hydrodynamic shear stress experienced at the well-fluid interface increases as the $3/2$ power of the rotation speed [33], we conclude that the aggregation growth rate increases linearly with the average wall shear stress on the orbital shaker. An explanation can be that agitation induces the release of μm -sized aggregates from the material surface into the solution thus allowing more aggregates to grow on the surface that has been shed or on secondary nucleation sites originating from fragmentation of growing fibrils [18].

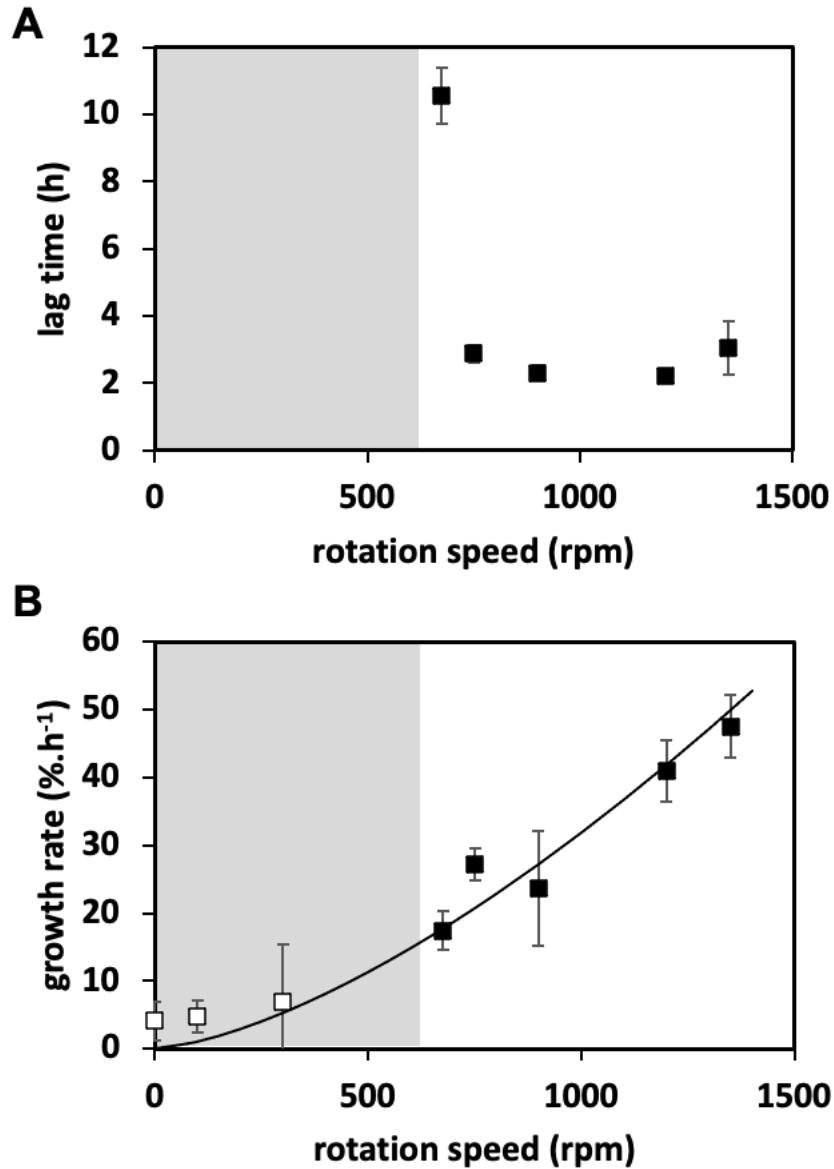


Figure 2: Effect of agitation on insulin aggregation kinetics. A: Effect of agitation on the insulin aggregation lag time. An insulin solution was agitated at 37°C, pH 7.4, in a hydrophobic polystyrene multi-well microplate, at the indicated rotation speeds. Insulin aggregation was monitored using optical density at 600 nm and the lag time was determined as explained in Materials and Methods. The grey region defines rotation speeds insufficient to ensure mixing of the solution. B: Effect of agitation on the insulin aggregation growth rate. Black squares: an insulin solution was agitated at 37°C, pH 7.4, in a hydrophobic polystyrene multi-well microplate, at the indicated rotation speed. White squares: an insulin solution was agitated at 37°C, pH 7, in a hydrophobic polystyrene multi-well microplate, at 1200 rpm for 2 hours, then the agitation was pursued at the indicated rotation speed. Insulin aggregation was monitored using optical density at 600 nm and the growth rate is expressed as the percentage of insulin aggregated per hour. The solid line represents the fit of the data with the equation 1, which indicates that the growth rate is proportional to the average wall shear stress in an orbital shaker [33]. Error bars can be smaller than the symbols. The raw data and data analysis are documented in Supplementary Materials.

Effect of the creation of dynamic triple interfaces on beads on insulin aggregation kinetics

Besides mixing and shear stress, agitation can have an additional effect: it creates dynamic triple solid-liquid-air interfaces, regions where the local concentration of adsorbed proteins is high and where these proteins are exposed to air [21]. Using the setup presented in **Figure 1**, we compared at even shear stress, the insulin aggregation kinetics in the presence and absence of dynamic triple interfaces. We performed two different experimental conditions: on one hand, a defined liquid volume was moved back and forth through the entire bead volume in the column so that triple interfaces were periodically created at the bead surfaces (intermittent wetting, **Figure 3A**); on the other hand, the same liquid volume was displaced above the bead volume so that the beads remained always immersed (permanent wetting, **Figure 3B**). One should note that the surface area swept by the liquid in the setup permitting intermittent wetting is 2.5 times higher than the surface in the setup in which the beads are always wet. By comparing the insulin aggregation kinetics of these two experimental conditions, it is possible to distinguish the effect of dynamic triple interfaces and the hydrodynamic shear stress which affects surface-adsorbed proteins.

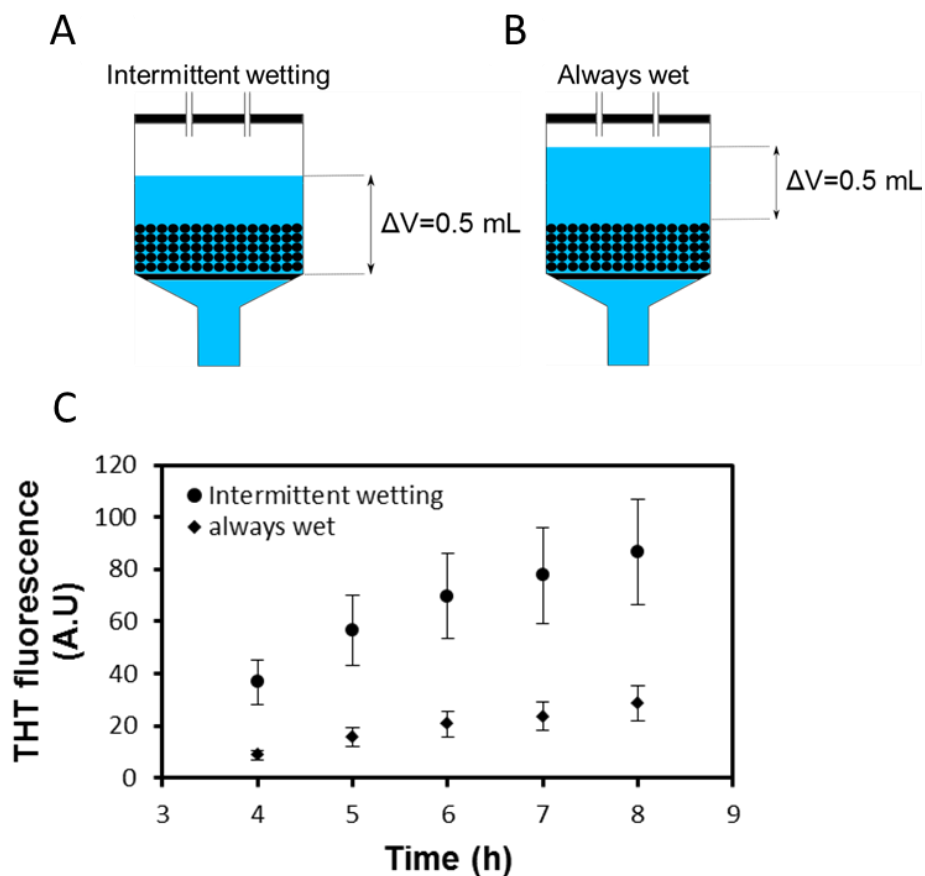


Figure 3: Influence of dynamic triple interfaces on insulin aggregation kinetics. A and B: Schematic views of the experimental setups. The insulin solution is represented in blue, the column bed support (beneath the beads) in black, and the beads by black disks. ΔV represents the displaced liquid volume and the displacement zone is indicated by a double-headed arrow. A: intermittent wetting. The entire bead volume is repeatedly filled then completely emptied, resulting in the creation of dynamic triple interfaces at the surface of each bead. B: permanent wetting. The solution meniscus always remains above the beads so that no dynamic triple interfaces are created on the beads. C: insulin aggregation kinetics in the presence (circles, intermittent wetting) and in the absence (diamonds, always wet) of dynamic triple interfaces, at equivalent shear stress. ThT fluorescence is measured simultaneously for both conditions starting when they reach a significant value (4 hours). Data points represent the mean values and error bars the standard deviation of three independent experiments.

In the intermittent wetting condition (circles on **Figure 3C**), the ThT fluorescence increases linearly between 5 and 8 hours at a rate of 9.8 ± 2.3 A.U. per hour. When beads remain immersed (diamonds on **Figure 3C**), the ThT fluorescence increases linearly at a rate of 4.2 ± 1.0 A.U. per hour. The aggregation speed is thus 2.3 times faster for the intermittent wetting condition compared to the other condition. This indicates that the formation of insulin aggregates is commensurate with the amount of triple interfaces created through sweeping of the protein solution over solid surfaces.

This experiment shows the accelerating effect of the presence of dynamic triple interfaces on insulin aggregation. Indeed, at equivalent shear stress the number of insulin aggregates created increases with the amount of triple interface surface available. One possible explanation could be that insulin molecules adsorbed at dynamic triple interfaces become unfolded and aggregate due to dehydration stress induced by intermittent exposure to air similarly to what was observed by Frachon *et al.* [21]. Another possible mechanism is that insulin, adsorbed at the air-solution interface, aggregates due to interfacial compression/expansion when the solution passes through the beads and these aggregates are then deposited on the hydrophobic beads.

Effect of the liquid sweeping speed on insulin aggregation kinetics

When the liquid is withdrawn from the column, the bead surface is swept by the solution meniscus, creating moving triple interfaces. One could imagine that the speed at which the meniscus sweeps the surface can be of importance in the aggregation process. We designed experiments (**Figure 4**) in which the flow rates and thus the shear stresses are different albeit conserving the same total number of full/empty column cycles in order to compare identical amounts of dynamic triple interfaces. In the fast-sweeping condition, the flow rate is twice higher than in the slow sweeping condition, which is achieved by pump synchronization introducing waiting times (**Figure 4B**). Both pumps are started simultaneously and fill the columns with 0.5 mL of insulin solution. In the fast-sweeping condition, the column is filled twice faster so a waiting time is set until the end of the filling of the column with the slow sweeping condition. Then, both pumps initiate the emptying of the columns simultaneously. Again, the column is emptied faster in the fast-sweeping condition so another waiting time is introduced until the column with the slower flow rate is empty. When both columns are empty, a new pumping cycle begins. With this pump program, the column fill/empty cycles have the same overall duration.

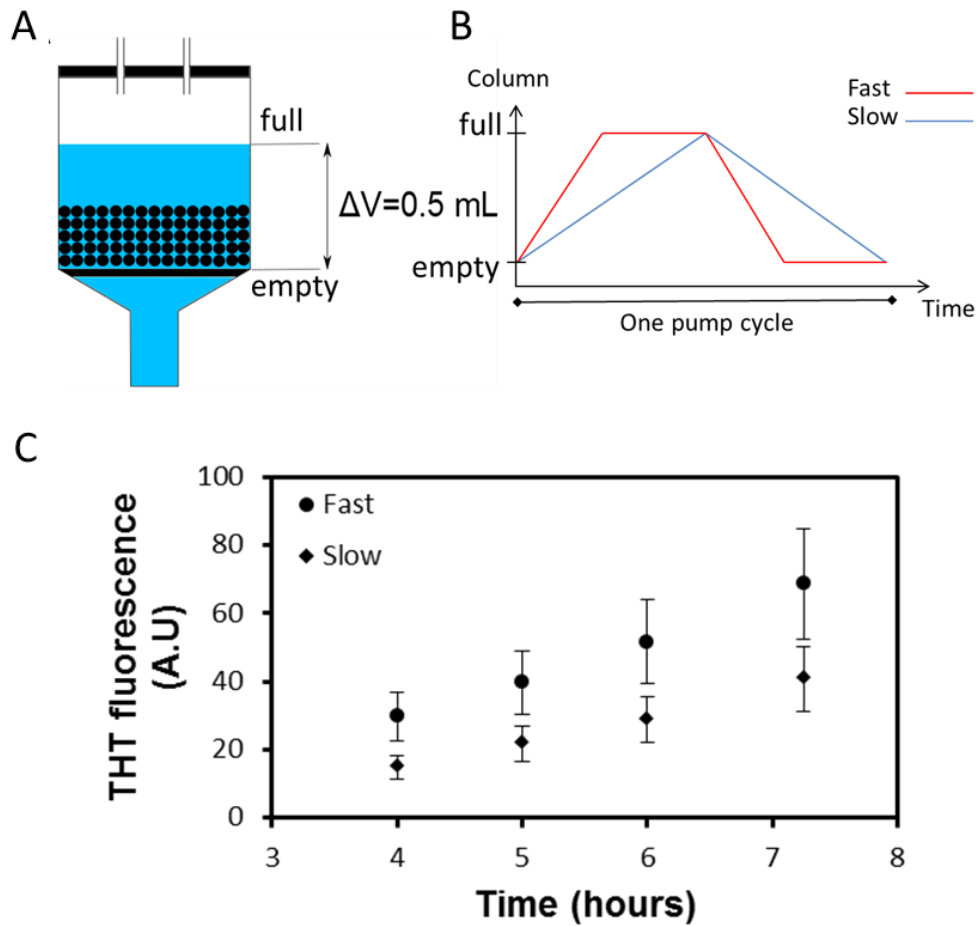


Figure 4: Influence of the flow rate on insulin aggregation kinetics. A: Schematic view of the experimental conditions. The insulin solution is represented in blue, the column bed support (beneath the beads) in black, and the beads by black disks. ΔV represents the displaced liquid volume. B: pump cycle description. The ordinate axis represents the filling state of the column. The pump programs of the slow and fast sweeping conditions are represented in blue and red, respectively. The flow rate is set to 4 mL/min for the fast-sweeping condition and to 2 mL/min for the slow sweeping one. C: insulin aggregation kinetics in the fast (circles) and slow (diamonds) sweeping conditions, at equivalent total number of pumping cycles. ThT fluorescence is measured simultaneously for both conditions starting when they reach a significant value (4 hours). Data points represent the mean values and error bars the standard deviation of three independent experiments.

After 4 hours, the ThT fluorescence signal increases linearly with time in both conditions (**Figure 4C**). The insulin aggregation kinetics in the fast-sweeping condition seems to be globally faster. Indeed, at any given time, its ThT fluorescence is almost twice higher, than the one in the slow sweeping condition. The growth rates are 12.9 ± 3.0 and 8.5 ± 2.0 A.U. per hour for the fast and slow sweeping conditions, respectively. Thus, the insulin aggregation kinetics in the fast-sweeping condition seems to be faster. However, the growth rate differences are not statistically significant, probably due to the small difference in sweeping speeds.

This experiment was designed to assess the effect of hydrodynamic shear stress (induced by increased flow rate) in the presence of dynamic triple interfaces. Similar to the interpretation given for the first experiment (**Figure 2**), shear stress tends to detach aggregates adsorbed at the triple interfaces, leaving room for new aggregate formations, and to break adsorbed fibrils, potentially triggering secondary nucleation in the bulk solution [34]. Both those mechanisms can lead to an increased aggregation kinetics observed here. However, the modest difference between slow and high-flow rates implies that shear stress has a relatively moderate effect compared to the presence of dynamic triple interfaces *per se*.

It should also be noted that the beads located at the bottom of the column spend a longer time in a dry state in the fast-sweeping condition than in the slow one. This could potentially have an effect on the insulin aggregation kinetics but, with the setup on **Figure 4**, it is difficult to study separately the effect of the sweeping speed and the drying time of the hydrophobic surface.

Aggregation on a rod: early formation of ThT-positive aggregates at the triple interface

In order to directly observe solid-liquid-air interfaces at the early stage of aggregation, we created an experimental setup in which hydrophobic, silanized glass rods are plunged in an insulin solution inside an agitated hydrophilic microplate (**Figure 5A**). In this setup, despite the strong agitation (1200 rpm), no significant ThT fluorescence could be observed in solution during the duration of the experiment (up to 6 hours of incubation) and only overnight experiments could show ThT fluorescence in solution. This low tendency to aggregate is due to the fact that the amount of hydrophobic solid surface (which exclusively comes from the rod) is greatly reduced compared to the one from a typical aggregation assay in hydrophobic wells (25 and 188 mm² for similar solution volumes, respectively).

After various incubation times, rods were taken and imaged under a fluorescence microscope (**Figure 5B**) where the presence of ThT-positive aggregates adsorbed on the rods can directly be assessed. The fluorescence intensity of every rod (n=24 for each incubation time) was then averaged and plotted on a graph (**Figure 5C and Supplementary materials**).

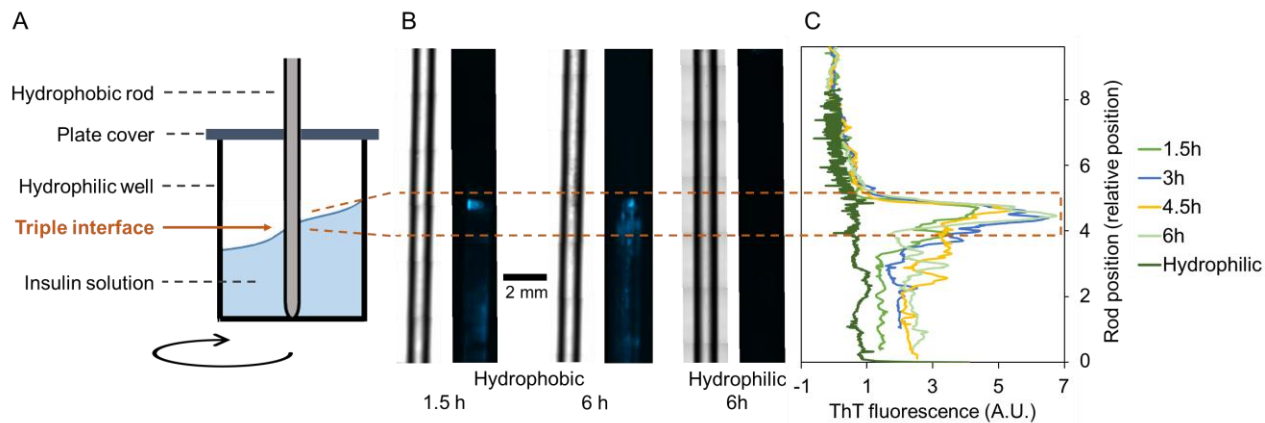


Figure 5: Aggregation of insulin is triggered at the dynamic triple line. A: Scheme of the experimental setup with a glass rod plunged inside a well, filled with 250 μL of insulin (86 μM) and ThT (20 μM) in TN buffer (pH 7.4). The multiwell plate was placed at 37°C and agitated at 1200 rpm during the duration of the experiment (up to 6h). B: Examples of representative hydrophobic or hydrophilic rods taken at two time points (1.5 h and 6 h) imaged under bright field (left image) and ThT fluorescence (right image). The hydrophilic rod experiment is given as an aggregation negative control. C: Localization of the ThT fluorescence on the rods' longitudinal axis in function of incubation time. 24 rods were analyzed per time point for the hydrophobic rods and 8 for the hydrophilic rod experiment (incubation of 6 h). The red dashed rectangle represents the location of the triple interface.

While there is no fluorescence in solution, the presence of a significant amount of ThT-positive aggregates, adsorbed on rods after just 1.5 h of incubation, can be detected. This observation is specific to hydrophobic rods since hydrophilic (PEGylated) rods do not show any sign of aggregation on their surface during the same timescale (**Fig. 5B and C**). ThT-positive aggregates can be found randomly dispersed on all the immersed section of the rods. To take into account the presence of these random aggregation spots, a large number of replicas was performed (24 rods per time point). For each rod, three areas can be distinguished, namely, the never immersed area, the intermittently immersed area, and the always immersed area. Mean fluorescence intensities and standard deviations were calculated for each area and each time point (Supplementary Materials). For a given area, mean fluorescence intensities are very similar for all time points considered. However, clear differences can be seen between areas (e.g. at 3 h, 0.3 ± 0.9 , 6.6 ± 3.9 , and 2.0 ± 0.7 A.U., for the never immersed, intermittently immersed and always immersed areas, respectively). The variability of the fluorescence values is high in the intermittently and always immersed areas, due to the presence of sporadic aggregation spots. However, there is a clear fluorescence accumulation in the intermittently immersed area (extending over approximately 1 mm), corresponding to the solid-liquid-air interface. The overall shape of the fluorescence distributions at the different time points (Figure 5C) does not change, eliminating the possibility of aggregate desorption followed by rapid re-adsorption on other areas

of the rod. This experiment strongly points out that the intermittently wet triple interface, where the air, the hydrophobic glass rod, and the protein solution meet, is a preferential place where aggregation can start. The shear stress and the solution mixing being identical all along the hydrophobic glass rod, it seems that the meniscus movement over the hydrophobic glass rod triggers insulin aggregation, potentially by exposing adsorbed proteins to air or by concentrating deposited aggregates from the air-solution interface.

Discussion

The kinetic experiments done in hydrophobic microplates showed that insulin stability is particularly sensitive to agitation. First, solution mixing provides a constant amount of insulin molecules to interact with the interfaces and with already adsorbed proteins, promoting nucleation and sustaining the formation of insulin aggregates [35]. Indeed, since pre-nuclei complexes are extremely unstable [36], an insufficient supply of native molecules to the nucleation site could increase the scarcity of a nucleation event. Secondly, during the growth of insulin oligomers, hydrodynamic shear stress can break or remove the larger molecular weight structures [37], thus triggering secondary nucleation sites for insulin aggregation [20]. Then, the growth rate of aggregates increases with the shear stress which can correspond either to a growth of the aggregates *per se* but perhaps also to a more efficient tearing of surface-adsorbed aggregates into the solution.

It is now well documented that nucleation is usually the limiting step during amyloid formation [34,38]. The present experiments confirm this observation and show that mixing, and not shear stress, is responsible for the onset of aggregation during agitation. The effect of shear stress on protein denaturation or conformational change is often refuted in the literature, at least at the molecular level on the basis of the low scales of fluid mechanical forces applied on nanometric objects [39,40]. However, during the growth phase, micrometric aggregates could indeed be affected by shear stress and for instance be detached from the surface to be released into the solution. Indeed, the minimal size of the insulin aggregates which can be detached by shear stress of this order is 200 nm as observed by Dathe *et al.* [41].

We have designed an experimental setup (**Figure 1**) which allows to test the effect of a sweeping air-liquid interface on bead-adsorbed proteins. This setup can easily be run in parallel on multiple

columns with beads made of different materials using a multi-channel fluidic inlet and proper tubing. It can be combined with different readout modalities allowing to record pertinent parameters (e.g. fluorescence, absorbance etc.). We have used it to investigate the mechanisms behind the role of agitation on surface-triggered insulin aggregation. The presence of intermittently wet hydrophobic surfaces appeared as a strong accelerator of insulin aggregation, independently of the hydrodynamic shear stress applied.

Besides dehydration of adsorbed proteins, other effects of agitation resulting from a dynamic air-liquid interface have been frequently suggested to trigger protein aggregation: for instance, foaming is known for its detrimental effects on the stability of proteins [42,43]. Moreover the formation of cavitation bubbles by ultra-sonication has been proposed as a primary nucleation-triggering mechanism [26,44,45]. In our case however, neither of the experimental setups resulted in the formation of foaming nor bubbles. It is then the dehydration of surface-adsorbed proteins, which is linked to the extent of the area swept by the dynamic triple interface that accelerates insulin aggregation. This result is in agreement with Duerkop *et al.* [39] who managed to study separately the two main components of cavitation (namely, increase of vapor/liquid interface and high shear stress) and showed that the increased amount of vapor/liquid interfaces was the driving force of protein aggregation during cavitation.

Finally, we have mapped the distribution of early ThT-positive aggregates on the surface of hydrophobic rods in an agitated insulin solution (**Figure 5**). The permanently immersed surfaces were sporadically covered by fluorescent objects while the surfaces located on the dynamic triple line displayed a striking coverage of ThT fluorescence showing the preferential formation of early aggregates on an intermittently dehydrated surface. This is in good agreement with previous studies **which** showed the existence of a synergistic effect of the combined presence of a triple interface and agitation for the aggregation of several proteins such as antibodies, insulin, and lysozyme [18,40,46]. However, this rules out the scenario where insulin aggregates would form homogeneously on the immersed hydrophobic surface and would subsequently be detached by the sweeping of the meniscus, as described by Gerhardt *et al.* [46]. In contrast, this result demonstrates that insulin molecules preferentially unfold and aggregate at the dynamic triple line because of the dehydration stress induced by intermittent wetting (**Figure 6**).

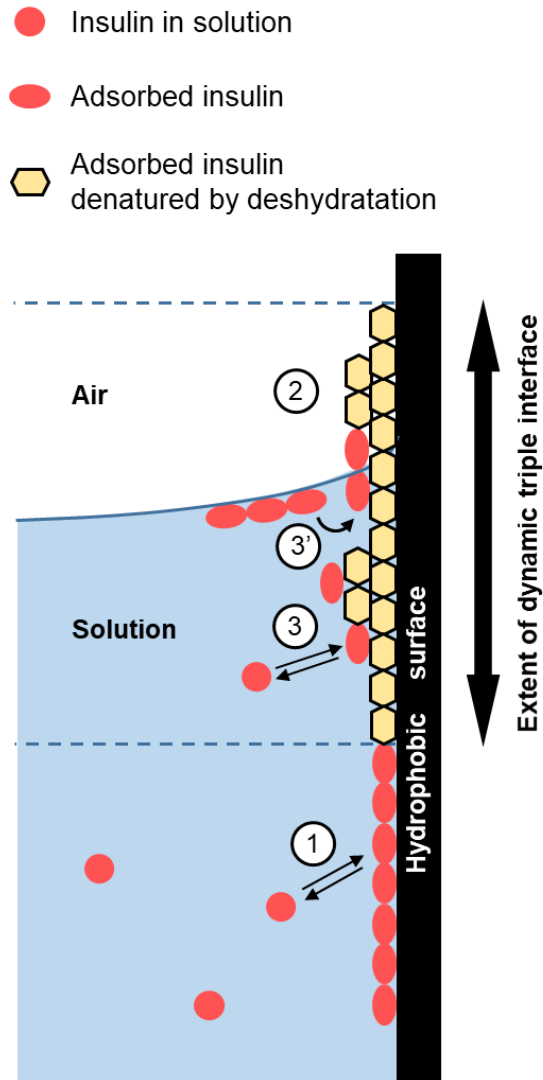


Figure 6: Schematic illustrating the effect of a dynamic triple interface on insulin aggregation. Insulin molecules in solution (red circles) adsorb on the hydrophobic surface (1); when the adsorbed molecules (red ellipses) are exposed to air, they further unfold (yellow hexagons) by dehydration (2); new solution insulin molecules can then adsorb on this dehydrated layer (3); the deposition of insulin molecules previously adsorbed at the air-liquid interface is also possible (3'). This layer of denatured molecules can then become the preferential nucleation place. The extent of the dynamic triple interface is shown on the right by the double-headed arrow and its limits are indicated by dashed lines.

The adsorption and partial unfolding of insulin molecules on hydrophobic surfaces (**Figure 6.1**) is well documented [18,47,48], however the subsequent nucleation is a very stochastic process. Here, we propose a model in which the dehydration of this adsorbed layer (**Figure 6.2**), results in the formation of a denatured protein layer on top of which new native molecules can adsorb (**Figure 6.3**) and undergo dehydration at the next drying/wetting cycle. Concomitantly, the deposition of proteins adsorbed at the air-liquid interface directly on the hydrophobic surface or

on top of already adsorbed protein during the sweeping by the triple line (**Figure 6.3'**) could also explain the dependency on both hydrophobic surfaces and dynamic triple interfaces. This stacking of partially denatured protein eventually becomes the preeminent nucleation and growth place by comparison with the less favorable conditions occurring at the permanently immersed surface.

Conclusion

The present study, in agreement with previous literature, emphasizes the requirement for a combination of agitation and presence of hydrophobic surfaces in order to induce insulin aggregation in physiological conditions [18,23,27,49]. However, the precise role of these two factors is still not fully understood. In particular, there have been many discussions about the mechanisms at play during agitation. Here, we show that the hydrodynamic shear stress involved during agitation contributes to a lesser extent to insulin aggregation compared to the presence of dynamic solid-liquid-air interfaces. The prominence of dynamic hydrophobic interfaces relative to shear stress has already been observed for the primary nucleation of many aggregation-prone proteins [39,46]. In the case of insulin, this can be explained by the major role played by dehydration of adsorbed proteins that can cause insulin conformational changes favorable to aggregation [48].

Our findings also indicate that triple interfaces are strong preferential places where insulin aggregates start to form and from which they are subsequently shed by a sweeping meniscus and end up in solution. This result has practical implications in the pharmaceutical field. Indeed, despite being intrinsically unavoidable, pharmaceutical processes involving both an air-liquid interface and a hydrophobic solid-liquid interface, such as mixing or transport in hydrophobic containers, should thus be carefully monitored in order to avoid protein aggregation at dynamic triple interfaces.

CRedit author statement

KC: Formal analysis, Investigation, Methodology, Writing - original draft. **TF:** Formal analysis, Investigation, Methodology, Writing - original draft. **LM:** Conceptualization, Data curation,

Formal analysis, Investigation, Methodology, Validation, Writing - review & editing. **LN**: Formal analysis, Investigation, Methodology. **CV**: Conceptualization, Formal analysis, Funding acquisition, Investigation, Supervision, Writing - review & editing. Antoine Maze: Formal analysis, Investigation, Methodology. **FB**: Conceptualization, Data curation, Formal analysis, Funding acquisition, Project administration, Resources, Supervision, Validation, Writing - review & editing. **MW**: Conceptualization, Data curation, Formal analysis, Funding acquisition, Project administration, Resources, Supervision, Validation, Writing - review & editing

Acknowledgements

KC was a recipient of a PhD grant from the French Ministère de l'Enseignement Supérieur, de la Recherche et de l'Innovation. TF was a recipient of a Cifre PhD grant from ANRT. LN was a recipient of a PhD grant from the Macodev cluster of the French Région Auvergne Rhône-Alpes. CV is grateful for funding by the CNRS. We thank Léa Echard for excellent experimental assistance. We acknowledge the support of the center of excellence on Multifunctional Architected Materials "CEMAM" (Investissements d'avenir, ANR-10-LABX-44-1).

References

- [1] M.S. Kinch, An overview of FDA-approved biologics medicines, *Drug Discov. Today*. 20 (2015) 393–398. <https://doi.org/10.1016/j.drudis.2014.09.003>.
- [2] H.M. Shepard, G.L. Phillips, C.D. Thanos, M. Feldmann, Developments in therapy with monoclonal antibodies and related proteins, *Clin. Med. (Northfield. Ill)*. 17 (2017) 220–232. <https://doi.org/10.7861/clinmedicine.17-3-220>.
- [3] A.L. Grilo, A. Mantalaris, The Increasingly Human and Profitable Monoclonal Antibody Market, *Trends Biotechnol.* 37 (2019) 9–16. <https://doi.org/10.1016/j.tibtech.2018.05.014>.
- [4] W. Wang, S. Nema, D. Teagarden, Protein aggregation—Pathways and influencing factors, *Int. J. Pharm.* 390 (2010) 89–99. <https://doi.org/10.1016/j.ijpharm.2010.02.025>.
- [5] S. Mitragotri, P.A. Burke, R. Langer, Overcoming the challenges in administering biopharmaceuticals: formulation and delivery strategies, *Nat. Rev. Drug Discov.* 13 (2014) 655–672. <https://doi.org/10.1038/nrd4363>.
- [6] M.R. Nejadnik, T.W. Randolph, D.B. Volkin, C. Schöneich, J.F. Carpenter, D.J.A. Crommelin, W. Jiskoot, Postproduction Handling and Administration of Protein

- Pharmaceuticals and Potential Instability Issues, *J. Pharm. Sci.* 107 (2018) 2013–2019. <https://doi.org/10.1016/j.xphs.2018.04.005>.
- [7] J. Li, M.E. Krause, X. Chen, Y. Cheng, W. Dai, J.J. Hill, M. Huang, S. Jordan, D. LaCasse, L. Narhi, E. Shalaev, I.C. Shieh, J.C. Thomas, R. Tu, S. Zheng, L. Zhu, Interfacial Stress in the Development of Biologics: Fundamental Understanding, Current Practice, and Future Perspective, *AAPS J.* 21 (2019) 44. <https://doi.org/10.1208/s12248-019-0312-3>.
- [8] M.E.M. Cromwell, E. Hilario, F. Jacobson, Protein aggregation and bioprocessing, *AAPS J.* 8 (2006) E572–E579. <https://doi.org/10.1208/aapsj080366>.
- [9] W. Norde, My voyage of discovery to proteins in flatland ...and beyond, *Colloids Surfaces B Biointerfaces.* 61 (2008) 1–9. <https://doi.org/10.1016/j.colsurfb.2007.09.029>.
- [10] K. Nakanishi, T. Sakiyama, K. Imamura, On the adsorption of proteins on solid surfaces, a common but very complicated phenomenon, *J. Biosci. Bioeng.* 91 (2001) 233–244. [https://doi.org/10.1016/S1389-1723\(01\)80127-4](https://doi.org/10.1016/S1389-1723(01)80127-4).
- [11] M. Rabe, D. Verdes, S. Seeger, Understanding protein adsorption phenomena at solid surfaces, *Adv. Colloid Interface Sci.* 162 (2011) 87–106. <https://doi.org/10.1016/j.cis.2010.12.007>.
- [12] S. Rudiuk, L. Cohen-Tannoudji, S. Huille, C. Tribet, Importance of the dynamics of adsorption and of a transient interfacial stress on the formation of aggregates of IgG antibodies, *Soft Matter.* 8 (2012) 2651. <https://doi.org/10.1039/c2sm07017k>.
- [13] M. Kastantin, B.B. Langdon, D.K. Schwartz, A bottom-up approach to understanding protein layer formation at solid–liquid interfaces, *Adv. Colloid Interface Sci.* 207 (2014) 240–252. <https://doi.org/10.1016/j.cis.2013.12.006>.
- [14] E. Koepf, S. Eisele, R. Schroeder, G. Brezesinski, W. Friess, Notorious but not understood: How liquid-air interfacial stress triggers protein aggregation, *Int. J. Pharm.* 537 (2018) 202–212. <https://doi.org/10.1016/j.ijpharm.2017.12.043>.
- [15] J. Wiesbauer, R. Prassl, B. Nidetzky, Renewal of the Air–Water Interface as a Critical System Parameter of Protein Stability: Aggregation of the Human Growth Hormone and Its Prevention by Surface-Active Compounds, *Langmuir.* 29 (2013) 15240–15250. <https://doi.org/10.1021/la4028223>.
- [16] L. Jean, C.F. Lee, D.J. Vaux, Enrichment of Amyloidogenesis at an Air-Water Interface,

- Biophys. J. 102 (2012) 1154–1162. <https://doi.org/10.1016/j.bpj.2012.01.041>.
- [17] A.S. Sediq, R.B. van Duijvenvoorde, W. Jiskoot, M.R. Nejadnik, No Touching! Abrasion of Adsorbed Protein Is the Root Cause of Subvisible Particle Formation During Stirring, *J. Pharm. Sci.* 105 (2016) 519–529. <https://doi.org/10.1016/j.xphs.2015.10.003>.
- [18] F. Grigolato, C. Colombo, R. Ferrari, L. Rezabkova, P. Arosio, Mechanistic Origin of the Combined Effect of Surfaces and Mechanical Agitation on Amyloid Formation, *ACS Nano*. 11 (2017) 11358–11367. <https://doi.org/10.1021/acs.nano.7b05895>.
- [19] S.A. McBride, S.P. Sanford, J.M. Lopez, A.H. Hirsra, Shear-induced amyloid fibrillization: the role of inertia, *Soft Matter*. 12 (2016) 3461–3467. <https://doi.org/10.1039/C5SM02916C>.
- [20] M. Törnquist, T.C.T. Michaels, K. Sanagavarapu, X. Yang, G. Meisl, S.I.A. Cohen, T.P.J. Knowles, S. Linse, Secondary nucleation in amyloid formation, *Chem. Commun.* 54 (2018) 8667–8684. <https://doi.org/10.1039/C8CC02204F>.
- [21] T. Frachon, F. Bruckert, Q. Le Masne, E. Monnin, M. Weidenhaupt, Insulin Aggregation at a Dynamic Solid–Liquid–Air Triple Interface, *Langmuir*. 32 (2016) 13009–13019. <https://doi.org/10.1021/acs.langmuir.6b03314>.
- [22] M.I. Ivanova, S.A. Sievers, M.R. Sawaya, J.S. Wall, D. Eisenberg, Molecular basis for insulin fibril assembly, *Proc. Natl. Acad. Sci.* 106 (2009) 18990–18995. <https://doi.org/10.1073/pnas.0910080106>.
- [23] V. Sluzky, J.A. Tamada, A.M. Klibanov, R. Langer, Kinetics of insulin aggregation in aqueous solutions upon agitation in the presence of hydrophobic surfaces., *Proc. Natl. Acad. Sci.* 88 (1991) 9377–9381. <https://doi.org/10.1073/pnas.88.21.9377>.
- [24] D.F. Waugh, A Fibrous Modification of Insulin. I. The Heat Precipitate of Insulin, *J. Am. Chem. Soc.* 68 (1946) 247–250. <https://doi.org/10.1021/ja01206a030>.
- [25] K. Irsigler, H. Kritz, Long-Term Continuous Intravenous Insulin Therapy with a Portable Insulin Dosage-regulating Apparatus, *Diabetes*. 28 (1979) 196–203. <https://doi.org/10.2337/diab.28.3.196>.
- [26] H. Wu, S. Movafaghi, I.M. Francino Urdániz, T.M. Rowe, A. Goodwin, T.W. Randolph, Insulin Fibril Formation Caused by Mechanical Shock and Cavitation, *J. Phys. Chem. B*. 125 (2021) 8021–8027. <https://doi.org/10.1021/acs.jpcc.1c01997>.
- [27] T. Ballet, F. Bruckert, P. Mangiagalli, C. Bureau, L. Boulangé, L. Nault, T. Perret, M.

- Weidenhaupt, DnaK Prevents Human Insulin Amyloid Fiber Formation on Hydrophobic Surfaces, *Biochemistry*. 51 (2012) 2172–2180. <https://doi.org/10.1021/bi201457u>.
- [28] J. Moeller, A.K. Denisin, J.Y. Sim, R.E. Wilson, A.J.S. Ribeiro, B.L. Pruitt, Controlling cell shape on hydrogels using lift-off protein patterning, *PLoS One*. 13 (2018) e0189901. <https://doi.org/10.1371/journal.pone.0189901>.
- [29] K. Chouchane, C. Vendrely, M. Amari, K. Moreaux, F. Bruckert, M. Weidenhaupt, Dual Effect of (LK)_nL Peptides on the Onset of Insulin Amyloid Fiber Formation at Hydrophobic Surfaces, *J. Phys. Chem. B*. 119 (2015) 10543–10553. <https://doi.org/10.1021/acs.jpcc.5b07365>.
- [30] C.A. Schneider, W.S. Rasband, K.W. Eliceiri, NIH Image to ImageJ: 25 years of image analysis, *Nat. Methods*. 9 (2012) 671–675. <https://doi.org/10.1038/nmeth.2089>.
- [31] O. Hoyer, A. Vester, R. Pätzold, Optimization of mixing parameters in lab automation for high & low sample volumes Temperature Control & Mixing made easy, 2012.
- [32] J. Büchs, U. Maier, S. Lotter, C.P. Peter, Calculating liquid distribution in shake flasks on rotary shakers at waterlike viscosities, *Biochem. Eng. J.* 34 (2007) 200–208. <https://doi.org/10.1016/j.bej.2006.12.005>.
- [33] R.E. Berson, M.R. Purcell, M.K. Sharp, Computationally Determined Shear on Cells Grown in Orbiting Culture Dishes, in: *Oxyg. Transp. to Tissue XXIX*, Springer US, Boston, MA, MA, 2008: pp. 189–198. https://doi.org/10.1007/978-0-387-74911-2_22.
- [34] F. Grigolato, P. Arosio, The role of surfaces on amyloid formation, *Biophys. Chem.* 270 (2021) 106533. <https://doi.org/10.1016/j.bpc.2020.106533>.
- [35] K. Chouchane, I. Pignot-Paintrand, F. Bruckert, M. Weidenhaupt, Visible light-induced insulin aggregation on surfaces via photoexcitation of bound thioflavin T, *J. Photochem. Photobiol. B Biol.* 181 (2018) 89–97. <https://doi.org/10.1016/j.jphotobiol.2018.02.025>.
- [36] C.-T. Lee, E.M. Terentjev, Mechanisms and rates of nucleation of amyloid fibrils, *J. Chem. Phys.* 147 (2017) 105103. <https://doi.org/10.1063/1.4995255>.
- [37] I.B. Bekard, P. Asimakis, J. Bertolini, D.E. Dunstan, The effects of shear flow on protein structure and function, *Biopolymers*. 95 (2011) n/a-n/a. <https://doi.org/10.1002/bip.21646>.
- [38] Z.L. Almeida, R.M.M. Brito, Structure and aggregation mechanisms in amyloids, *Molecules*. 25 (2020). <https://doi.org/10.3390/molecules25051195>.
- [39] M. Duerkop, E. Berger, A. Dürauer, A. Jungbauer, Impact of Cavitation, High Shear Stress

- and Air/Liquid Interfaces on Protein Aggregation, *Biotechnol. J.* 13 (2018) 1800062. <https://doi.org/10.1002/biot.201800062>.
- [40] F. Grigolato, P. Arosio, Synergistic effects of flow and interfaces on antibody aggregation, *Biotechnol. Bioeng.* 117 (2020) 417–428. <https://doi.org/10.1002/bit.27212>.
- [41] M. Dathe, K. Gast, D. Zirwer, H. Welfle, B. Mehlis, Insulin aggregation in solution, *Int. J. Pept. Protein Res.* 36 (2009) 344–349. <https://doi.org/10.1111/j.1399-3011.1990.tb01292.x>.
- [42] Y.-F. Maa, C.C. Hsu, Protein denaturation by combined effect of shear and air-liquid interface, *Biotechnol. Bioeng.* 54 (1997) 503–512. [https://doi.org/10.1002/\(SICI\)1097-0290\(19970620\)54:6<503::AID-BIT1>3.0.CO;2-N](https://doi.org/10.1002/(SICI)1097-0290(19970620)54:6<503::AID-BIT1>3.0.CO;2-N).
- [43] C.R. Thomas, D. Geer, Effects of shear on proteins in solution, *Biotechnol. Lett.* 33 (2011) 443–456. <https://doi.org/10.1007/s10529-010-0469-4>.
- [44] H. Muta, Y.-H. Lee, J. Kardos, Y. Lin, H. Yagi, Y. Goto, Supersaturation-limited Amyloid Fibrillation of Insulin Revealed by Ultrasonication, *J. Biol. Chem.* 289 (2014) 18228–18238. <https://doi.org/10.1074/jbc.M114.566950>.
- [45] K. Nakajima, D. Nishioka, M. Hirao, M. So, Y. Goto, H. Ogi, Drastic acceleration of fibrillation of insulin by transient cavitation bubble, *Ultrason. Sonochem.* 36 (2017) 206–211. <https://doi.org/10.1016/j.ultsonch.2016.11.034>.
- [46] A. Gerhardt, N.R. McGraw, D.K. Schwartz, J.S. Bee, J.F. Carpenter, T.W. Randolph, Protein Aggregation and Particle Formation in Prefilled Glass Syringes, *J. Pharm. Sci.* 103 (2014) 1601–1612. <https://doi.org/10.1002/jps.23973>.
- [47] L. Nault, P. Guo, B. Jain, Y. Bréchet, F. Bruckert, M. Weidenhaupt, Human insulin adsorption kinetics, conformational changes and amyloidal aggregate formation on hydrophobic surfaces, *Acta Biomater.* 9 (2013) 5070–5079. <https://doi.org/10.1016/j.actbio.2012.09.025>.
- [48] D.L. Cheung, The air-water interface stabilizes α -helical conformations of the insulin B-chain, *J. Chem. Phys.* 151 (2019) 064706. <https://doi.org/10.1063/1.5100253>.
- [49] L. Nielsen, R. Khurana, A. Coats, S. Frokjaer, J. Brange, S. Vyas, V.N. Uversky, A.L. Fink, Effect of Environmental Factors on the Kinetics of Insulin Fibril Formation: Elucidation of the Molecular Mechanism, *Biochemistry.* 40 (2001) 6036–6046. <https://doi.org/10.1021/bi002555c>.

